Journal of Organometallic Chemistry 695 (2010) 2401–2409

Contents lists available at ScienceDirect

Journal of Organometallic Chemistry

journal homepage: www.elsevier.com/locate/jorganchem

Neutral and cationic cyclometallated Ir(III) complexes of anthra[1,2-*d*]-imidazole-6,11-dione-derived ligands: Syntheses, structures and spectroscopic characterisation

Andrew J. Hallett*, Benjamin D. Ward, Benson M. Kariuki, Simon J.A. Pope*

School of Chemistry, Main Building, Cardiff University, Museum Avenue, Cardiff CF10 3AT, United Kingdom

ARTICLE INFO

Article history:
Received 11 May 2010
Received in revised form
9 July 2010
Accepted 15 July 2010
Available online 23 July 2010

Keywords:
Iridium
Cyclometallated
Anthraquinone
Structures
Luminescence
DFT

ABSTRACT

The syntheses of two new ligands and five new heteroleptic cyclometallated Ir(III) complexes are reported. The ligands are based upon a functionalised anthra[1,2-*d*]imidazole-6,11-dione core giving LH^{1-3} incorporating a pendant pyridine, quinoline or thiophene unit respectively. Neutrally charged, octahedral complexes $[Ir(ppy)_2(L^{1-3})]$ are chelated by two cyclometallated phenylpyridine (ppy) ligands and a third, ancillary deprotonated ligand L^{1-3}, whilst cationic analogues could only be isolated for $[Ir(ppy)_2(LH^{1-2})][PF_6]$. X-ray crystal structures for $[Ir(ppy)_2(L^1)]$, $[Ir(ppy)_2(LH^1)][PF_6]$ and $[Ir(ppy)_2(L^2)]$ showed the complexes adopt a distorted octahedral coordination geometry, with the anthra[1,2-*d*]imidazole-6,11-dione ligands coordinating in a bidentate fashion. Preliminary DFT calculations revealed that for the complexes of LH^1 and LH^2 the LUMO is exclusively localized on the ancillary ligand, whereas the nature of the HOMO depends on the protonation state of the ancillary ligand, often being composed of both Ir(III) and phenylpyridine character. UV–vis. and luminescence data showed that the ligands absorb into the visible region *ca.* 400 nm and emit *ca.* 560 nm, both of which are attributed to an intra-ligand CT transition within the anthra[1,2-*d*]imidazole-6,11-dione core. The complexes display absorption bands attributed to overlapping ligand-centred and ^{1}MLCT-type electronic transitions, whilst only $[Ir(ppy)_2(L^2)]$ appeared to possess typical ^{3}MLCT behaviour ($\lambda_{em} = 616$ nm; $\tau = 96$ ns in aerated MeCN). The remaining complexes were generally visibly emissive ($\lambda_{em} \approx 560$–570 nm; $\tau < 10$ ns in aerated MeCN) with very oxygen-sensitive lifetimes more indicative of ligand-centred processes.

1. Introduction

Functionalised luminescent metal complexes have attracted significant attention because of their far-reaching applicability in a multitude of areas, in particular photovoltaics, LEDs, responsive probes and biological imaging [1]. Transition metal d^6 complexes based upon Ru(II), Re(I), Os(II) have been studied in great detail due to their inherent kinetic stability, relative ease of synthetic development and tunable optical properties [2]. In particular, cyclometalated Ir(III) complexes have also been intensely investigated in the last two decades due to their interesting and useful photoluminescent properties [3] which can also encompass emission from multiple excited states. The first report that OLEDs prepared with $[Ir(ppy)_3]$ ($ppy^- = 2$-phenylpyridine) (Fig. 1) have efficiencies of more that 80%, stimulated great interest in derivatised Ir(III) complexes [4]. Contextually, OLEDs based upon the benchmark tris (8-hydroxyquinolinato)aluminum (Alq_3) complex possess an electroluminescence efficiency (quantum yield) which is limited to a maximum of 25% [5], however, in comparison phosphorescence emitting cyclometalled Ir(III) complexes are much improved in terms of their internal quantum yield, which increases to a theoretical maximum of 100% [6].

Bridge-splitting reactions of dimeric $[(ppy)_2Ir(\mu\text{-}Cl)_2Ir(ppy)_2]$ with neutral ligands gives the monomeric cationic complexes $[Ir(C^N)_2(X^Y)]^+$, whereas with anionic ligands, neutral complexes $[Ir(C^N)_2(X^Y)]$ are obtained (Fig. 1).

Within OLED development, neutral iridium complexes have generally attracted much more interest than cationic species predominantly because, firstly, improved ease of OLED fabrication (thermal stability allows vapour deposition), and secondly, the absence of counter ions, which reduces time-delays between 'switch-on' and observed emission within display-related applications. Most neutral species, however, are limited to homoleptic tris-cyclometallated complexes, such as $[Ir(ppy)_3]$ and derivatives

* Corresponding authors. Tel.: +44(0) 29 20879316; fax: +44(0) 29 20874030.
E-mail addresses: hallettaj@cardiff.ac.uk (A.J. Hallett), popesj@cardiff.ac.uk (S.J.A. Pope).

0022-328X/$ – see front matter © 2010 Elsevier B.V. All rights reserved.
doi:10.1016/j.jorganchem.2010.07.017

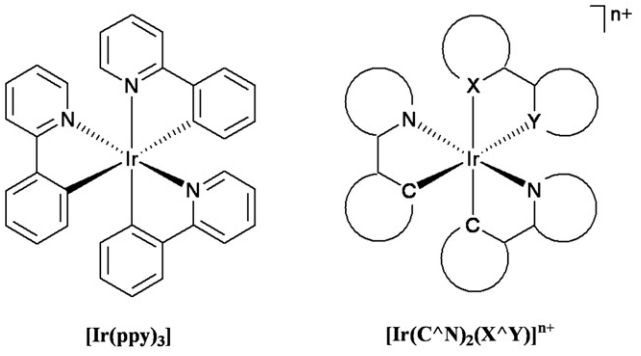

Fig. 1. The molecular structures of $[Ir(ppy)_3]$ and $[Ir(C^N)_2(X^Y)]^{n+}$.

thereof. Consequently, there have been a number of recent studies focusing on the synthetic development and resultant electronic effects of ancillary ligands [7]. The majority of these investigations, however, yielded cationic derivatives, which are predominantly used for electrochemiluminescence (ECL) [8]: inferior volatility [9] renders them less desirable for fabricated prototype OLED applications. Despite this certain OLEDs and solid light-emitting electrophosphorescent devices have been based on charged Ir(III) complexes, showing some promise because of enhanced charge transport properties that are mediated by the charged complex components [10].

In recent studies we have investigated the incorporation of substituted anthraquinone moieties into metal ion coordination complex architectures [11]. The reasons are two-fold: firstly, the optical properties of substituted anthraquinones can be invaluable in the design of complexes with interesting absorption and emission properties [12]; secondly, there is an extensive literature on the biological application of anthraquinone derivatives (both naturally occurring and synthetic), which encompass cytotoxic, anti-malarial and anti-cancer properties [13]. The biological activities are often related to the DNA targeting behaviour of substituted anthraquinones (the nature and positioning of the substitution can have a profound effect on the specific mode of binding) [14]. Chao and Ji and co-workers recently reported the cyclised derivatisation of 1,2-diaminoanthraquinone with 2-pyridinecarboxaldehyde giving a pyridine-appended anthra[1,2-*d*] imidazole-6,11-dione-derived ligand (LH^1) that can coordinate to Ru(II) giving a $[Ru(bpy)_2(L)]^{2+}$ type complex: studies have shown these compounds display DNA-binding behaviour *via* intercalation [15]. In this context, recent studies have also shown that an anthraquinone-tethered Pt(II) complex displays enhanced targeting and anti-cancer activity compared to *cis*-platin [16]. Emissive cyclometallated Ir(III) complexes have also shown great promise in sensor/probe development [17] and biological imaging applications, specifically at the cellular level, *via* confocal fluorescence microscopy [18].

We herein report the application of a synthesis [19] yielding two new anthraquinone-functionalised ligands LH^2 and LH^3. Together with the known ligand LH^1, we describe their complexation to bis-cyclometallated Ir(III) precursors giving synthetic control towards both neutral and cationic examples of heteroleptic Ir(III) complexes. The syntheses, structures and spectroscopic properties of the complexes are reported.

2. Experimental

2.1. General information

All reactions were performed with the use of vacuum line and Schlenk techniques. Reagents were commercial grade and were used without further purification. $[(ppy)_2Ir(\mu\text{-}Cl)_2Ir(ppy)_2]$ was prepared according to the literature procedure [20]. ^1H and $^{13}C\{^1H\}$ NMR spectra and were run on a NMR-FT Bruker 400 spectrometer and recorded in $CDCl_3$. ^1H and $^{13}C\{^1H\}$ NMR chemical shifts (δ) were determined relative to internal TMS and are given in ppm. Low-resolution mass spectra were obtained by the staff at Cardiff University. High-resolution mass spectra were carried out by the EPSRC National Mass Spectrometry Service at Swansea University. Infrared spectra were run on a Perkin–Elmer FT-1600 spectrophotometer as CH_2Cl_2 solutions. UV–vis studies were performed on a Jasco V-570 spectrophotometer as MeCN solutions (6.4×10^{-5} M^{-1}). Photophysical data were obtained on a JobinYvon-Horiba Fluorolog spectrometer fitted with a JY TBX picosecond photodetection module as MeCN solutions. Emission spectra were uncorrected and excitation spectra were instrument corrected. The pulsed source was a Nano-LED configured for 459 nm output operating at 500 or 100 kHz. Luminescence lifetime profiles were obtained using the JobinYvon-Horiba FluoroHub single photon counting module and the data fits yielded the lifetime values using the provided DAS9 deconvolution software.

2.2. Data collection and processing

Diffraction data for $[Ir(ppy)_2(L^1)]$, $[Ir(ppy)_2(L^2)]$ and $[Ir(ppy)_2(LH^1)][PF_6]$ were collected on a Nonius KappaCCD using graphite-monochromated Mo-Kα radiation ($\lambda = 0.71073$ Å) at 150 K. Software package Apex 2 (v2.1) was used for the data integration, scaling and absorption correction.

2.3. Structure analysis and refinement

The structure was solved by direct methods using SHELXS-97 and was completed by iterative cycles of ΔF-syntheses and full-matrix least squares refinement. All non-H atoms were refined anisotropically and difference Fourier syntheses were employed in positioning idealised hydrogen atoms and were allowed to ride on their parent C-atoms. All refinements were against F^2 and used SHELXL-97 [21].

2.4. Density functional theory

All calculations were performed on the Gaussian 03 program [22]. Geometry optimisations were carried out without geometry constraints using the B3PW91 functional. The LANL2DZ basis set was used for the Ir centres, and was invoked with pseudo-potentials for the core electrons, a 6-31G(d,p) basis set for all coordinating atoms with a 6-31G basis set for all remaining atoms. All optimisations were followed by frequency calculations to ascertain the nature of the stationary point (minimum or saddle point).

2.5. Synthesis of ligands

2.5.1. Ligand LH^1

Ligand LH^1 was prepared according to the literature procedure [19]. ^1H NMR data are as reported. IR (CH_2Cl_2) $\nu = 1607$(s), 1591(m) cm^{-1}. UV–vis (MeCN): λ_{max} (ε/dm^3 mol^{-1} cm^{-1}) = 392 (2800) nm.

2.5.2. Ligand LH^2

1,2-diaminoanthraquinone (0.385 g, 1.60 mmol) and 2-quinolinecarboxaldehyde (0.252 g, 1.60 mmol) were heated in nitrobenzene (10 ml) at 140 °C for 16 h. The mixture was allowed to cool and the product precipitated by the slow addition of Et_2O. The brown powder was filtered, washed with Et_2O and dried *in vacuo*. Yield = 0.553 g (1.48 mmol) 92%. ^1H NMR (400 MHz, $CDCl_3$) $\delta_H = 8.51$ (1H, d, $J_{HH} = 8.7$ Hz), 8.30 (3H, m), 8.22 (2H, m,), 8.16 (1H, d, $J_{HH} = 8.7$ Hz), 7.83 (1H, d, $J_{HH} = 8.8$ Hz), 7.78 (3H, m), 7.59 (1H, dd,

J_{HH} = 8.7 and 8.8 Hz) ppm. IR (CH_2Cl_2) ν = 1610(m), 1595(m) cm^{-1}. UV–vis (MeCN): λ_{max} (ε/dm^3 mol^{-1} cm^{-1}) = 393 (1600) nm. EI MS found *m/z* 375.1, calculated *m/z* 375.3 for $[M]^+$. HR MS found *m/z* 375.1002, calculated 375.1002 for $[C_{24}H_{13}O_2N_3]^+$.

2.5.3. Ligand LH^3

Prepared similarly from 1,2-diaminoanthraquinone (0.252 g, 1.06 mmol) and 2-thiophenecarboxaldehyde (0.1 ml, 1.07 mmol). Yield = 0.305 g (0.92 mmol) 87%. ^1H NMR (400 MHz, $CDCl_3$) δ_H = 8.27 (1H, d, J_{HH} = 8.7 Hz), 8.17 (2H, m), 7.99 (1H, d, J_{HH} = 8.4 Hz), 7.72 (3H, m), 7.52 (1H, d, J_{HH} = 4.7 Hz), 7.16 (1H, dd, J_{HH} = 4.7 and 8.7) ppm. IR (CH_2Cl_2) ν = 1606(m), 1588(s) cm^{-1}. UV–vis (MeCN): λ_{max} (ε/dm^3 mol^{-1} cm^{-1}) = 415 (19,100) nm. ES MS found *m/z* 331.1, calculated *m/z* 331.3 for $[M+H]^+$. HR MS found *m/z* 331.0528, calculated 331.0526 for $[C_{19}H_{11}O_2N_2S]^+$.

2.6. Synthesis of complexes

2.6.1. $[Ir(ppy)_2(L^1)]$

$[(ppy)_2Ir(\mu\text{-}Cl)_2Ir(ppy)_2]$ (0.050 g, 0.046 mmol), L^1 (0.031 g, 0.095 mmol) and Na_2CO_3 (0.010 g, 0.094 mmol) were heated at 120 °C in methoxyethanol (10 ml) for 16 h. The orange precipitate was filtered, wash with methoxyethanol (10 ml) and Et_2O (10 ml) and dried in *vacuo*. Yield = 0.056 g (0.068 mmol) 73%. ^1H NMR (400 MHz, $CDCl_3$) δ_H = 8.79 (1H, d, J_{HH} = 7.4 Hz), 8.27 (1H, d, J_{HH} = 7.4 Hz), 8.13 (1H, d, J_{HH} = 7.2 Hz), 7.71–7.86 (4H, m), 7.66 (1H, d, J_{HH} = 8.5 Hz), 7.45–7.63 (8H, m), 7.12 (1H, app. t, J_{HH} = 5.6 Hz){app. = apparent (coincident dd)}, 6.99 (1H, app. t, J_{HH} = 7.3 Hz), 6.92 (1H, app. t, J_{HH} = 7.3 Hz), 6.85 (2H app. t, J_{HH} = 7.3 Hz), 6.72 (2H, dd, J_{HH} = 7.3 and 7.2 Hz), 6.39 (2H, app. t, J_{HH} = 7.2 Hz), 6.32 (1H, d, J_{HH} = 8.5 Hz). IR (CH_2Cl_2) ν = 1608(s), 1584(m) cm^{-1}. UV–vis (MeCN): λ_{max} (ε/dm^3 mol^{-1} cm^{-1}) = 420 (12,600) nm. ES MS found *m/z* 826.2, calculated *m/z* 825.9 for $[M+H]^+$. HR MS found *m/z* 824.1771, calculated *m/z* 824.1765 for $[C_{42}H_{27}O_2N_5^{191}Ir]^+$.

2.6.2. $[Ir(ppy)_2(L^2)]$

Prepared similarly from $[(ppy)_2Ir(\mu\text{-}Cl)_2Ir(ppy)_2]$ (0.049 g, 0.046 mmol), LH^2 (0.035 g, 0.093 mmol) and Na_2CO_3 (0.010 g, 0.094 mmol). Yield = 0.061 g (0.070 mmol) 77%. ^1H NMR (400 MHz, $CDCl_3$) δ_H = 9.03 (1H, d, J_{HH} = 8.5 Hz), 8.31 (2H, app. t, J_{HH} = 8.8 Hz), 8.13 (1H, d, J_{HH} = 7.4 Hz), 7.32–7.78 (13H, m), 7.10 (1H, app. t, J_{HH} = 8.0 Hz), 7.02 (1H, app. t, J_{HH} = 7.8 Hz), 6.92 (2H, m), 6.81 (1H, app. t, J_{HH} = 7.4 Hz), 6.64 (2H, m), 6.49 (1H, d, J_{HH} = 6.7 Hz), 6.13 (1H, d, J_{HH} = 7.8 Hz), 6.06 (1H, d, J_{HH} = 8.8 Hz) ppm. IR (CH_2Cl_2) ν = 1606(s), 1584(m) cm^{-1}. UV–vis (MeCN): λ_{max} (ε/dm^3 mol^{-1} cm^{-1}) = 433 (15,300) nm. ES MS found *m/z* 876.2, calculated *m/z* 876.0 for $[M+H]^+$. HR MS found *m/z* 874.1939, calculated *m/z* 874.1922 for $[C_{46}H_{29}O_2N_5^{191}Ir]^+$.

2.6.3. $[Ir(ppy)_2(L^3)]$

Prepared similarly from $[(ppy)_2Ir(\mu\text{-}Cl)_2Ir(ppy)_2]$ (0.045 g, 0.042 mmol), LH^3 (0.029 g, 0.088 mmol) and Na_2CO_3 (0.010 g, 0.094 mmol). Yield = 0.047 g (0.057 mmol) 68%. ^1H NMR (400 MHz, $CDCl_3$) δ_H = 8.21 (1H, d, J_{HH} = 7.8 Hz), 8.03–8.16 (4H, m), 8.00 (1H, d, J_{HH} = 7.3 Hz), 7.52–7.77 (6H, m), 7.48 (1H, dd, J_{HH} = 7.7 and 7.5 Hz), 7.41 (1H, dd, J_{HH} = 7.8 and 7.5 Hz), 7.20 (1H, dd, J_{HH} = 7.8 and 7.3 Hz), 6.75–6.84 (3H, m), 6.70 (1H, dd, J_{HH} = 7.5 and 7.6 Hz), 6.48 (1H, app. t, J_{HH} = 7.5 Hz), 6.31 (1H, dd, J_{HH} = 7.6 and 7.3 Hz), 6.22 (2H, m), 6.09 (1H, d, J_{HH} = 7.5 Hz), 5.83 (1H, d, J_{HH} = 7.7 Hz) nm. ^{13}C-{^1H} NMR (101 MHz, $CDCl_3$) δ_C = 182.3, 180.8, 167.8, 166.9, 163.7, 152.8, 148.5, 147.0, 143.7, 143.1, 141.6, 137.9, 136.8, 136.0, 133.6, 132.8, 131.9, 131.2, 128.4, 126.3, 125.8, 124.8, 122.7, 121.2, 120.4, 119.1, 117.8, 117.5 ppm. IR (CH_2Cl_2) ν = 1608(s), 1587(s) cm^{-1}. UV–vis (MeCN): λ_{max} (ε/dm^3 mol^{-1} cm^{-1}) = 397 (13,200) nm. ES MS found *m/z* 831.2, calculated *m/z* 831.0 for $[M+H]^+$. HR MS found *m/z* 829.1384, calculated *m/z* 829.1377 for $[C_{41}H_{26}O_2N_4S^{191}Ir]^+$.

2.6.4. $[Ir(ppy)_2(LH^1)][PF_6]$

$[(ppy)_2Ir(\mu\text{-}Cl)_2Ir(ppy)_2]$ (0.040 g, 0.037 mmol) and LH^1 (0.025 g, 0.077 mmol) were heated at 120 °C in methoxyethanol (10 ml) for 16 h. The solvent was removed in *vacuo* and the crude product dissolved in MeCN (4 ml). NH_4PF_6 (0.983 g, 6.031 mmol) in water (1 ml) was added and stirred for 10 min. Water (20 ml) was then added and the product extracted with CH_2Cl_2 (2 × 10 ml). The combined organic phases were then washed with water (20 ml) and brine (20 ml) before being dried over $MgSO_4$. The solvent was reduced in volume (to *ca* 3 ml) and the product precipitated by the slow addition of Et_2O (20 ml). The product was then dried in vacuo. Yield = 0.057 g (0.058 mmol) 79%. ^1H NMR (400 MHz, $CDCl_3$) δ_H = 9.09 (1H, d, J_{HH} = 7.4 Hz), 8.03 (2H, dd, J_{HH} = 7.6 and 7.7 Hz), 7.91 (1H, d, J_{HH} = 7.2 Hz), 7.46–7.85 (12H, m), 7.30 (1H, dd, J_{HH} = 5.9 and 6.0 Hz), 7.02 (1H, app. t, J_{HH} = 7.4 Hz), 6.81–6.96 (5H, m), 6.47 (1H, d, J_{HH} = 8.6 Hz), 6.38 (1H, d, J_{HH} = 7.5 Hz), 6.28 (1H, d, J_{HH} = 7.4 Hz) ppm. ^{13}C-{^1H} NMR (101 MHz, $CDCl_3$) δ_C = 182.3, 181.5, 166.7, 159.3, 149.8, 149.6, 148.6, 147.9, 146.9, 145.8, 143.3, 142.9, 138.6, 136.9, 133.2, 132.9, 132.0, 131.5, 130.7, 129.7, 129.1, 127.3, 126.1, 125.5, 123.4, 122.3, 121.5, 120.6, 118.3, 118.1 ppm. IR (CH_2Cl_2) ν = 1609(s), 1584(m) cm^{-1}. UV–vis (MeCN): λ_{max} (ε/dm^3 mol^{-1} cm^{-1}) = 391 (16,100) nm. ES MS found *m/z* 826.2, calculated *m/z* 825.9 for $[M\text{-}PF_6]^+$. HR MS found *m/z* 824.1769, calculated *m/z* 824.1765 for $[C_{42}H_{27}O_2N_5^{191}Ir]^+$.

2.6.5. $[Ir(ppy)_2(LH^2)][PF_6]$

Prepared similarly from $[(ppy)_2Ir(\mu\text{-}Cl)_2Ir(ppy)_2]$ (0.040 g, 0.037 mmol) and LH^2 (0.030 g, 0.080 mmol). Yield = 0.050 g (0.049 mmol) 66%. ^1H NMR (400 MHz, $CDCl_3$) δ_H = 9.01 (1H, d, J_{HH} = 7.4 Hz), 8.43 (1H, d, J_{HH} = 7.6 Hz), 8.03–8.18 (3H, m), 7.40–7.81 (12H, m), 7.37 (1H, dd, J_{HH} = 7.2 and 7.6 Hz), 7.11 (1H, dd, J_{HH} = 7.9 and 7.7 Hz), 7.02 (1H, dd, J_{HH} = 7.4 and 7.6 Hz), 6.86–6.94 (2H, m), 6.82 (1H, dd, J_{HH} = 7.5 and 7.4 Hz), 6.77 (2H, br s), 6.42 (1H, d, J_{HH} = 7.2 Hz), 6.18 (1H, d, J_{HH} = 7.6 Hz), 6.12 (1H, d, J_{HH} = 8.7 Hz) ppm. IR (CH_2Cl_2) ν = 1608(s), 1585(s) cm^{-1}. UV–vis (MeCN): λ_{max}(ε/dm^3 mol^{-1} cm^{-1}) = 390 (23,300) nm. ES MS found *m/z* 876.2, calculated *m/z* 876.0 for $[M\text{-}PF_6]^+$. HR MS found *m/z* 874.1926, calculated *m/z* 874.1922 for $[C_{46}H_{29}O_2N_5^{191}Ir]^+$.

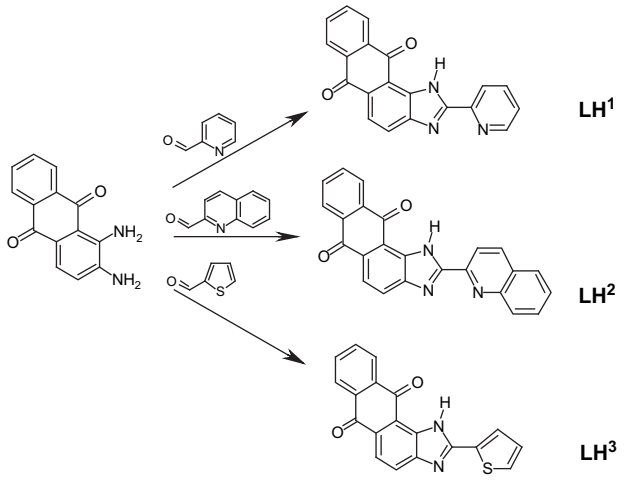

Scheme 1. The anthra[1,2-*d*]imidazole-6,11-dione-derived ligands used in this study.

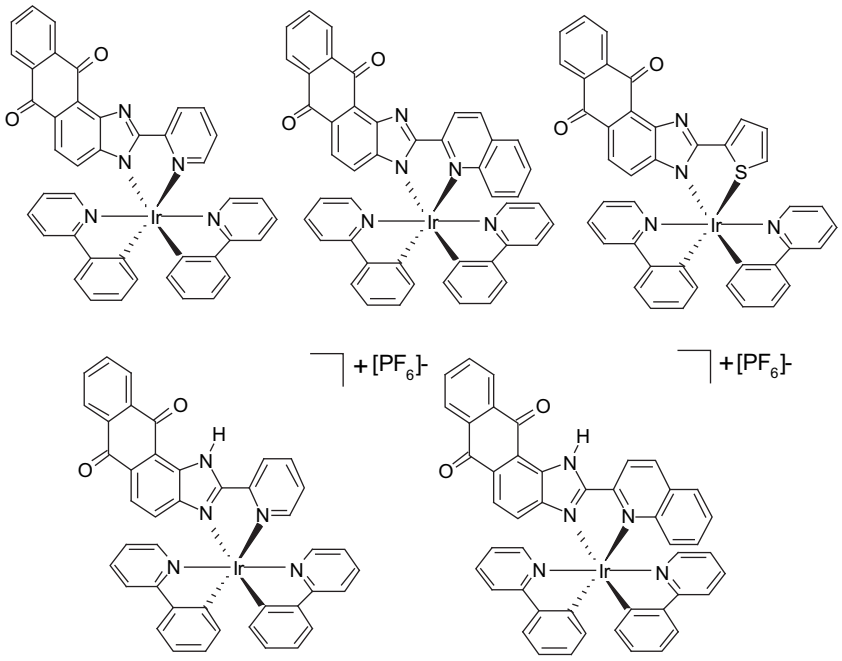

Fig 2. Proposed binding modes for the cyclometallated Ir(III) complexes isolated in this study.

3. Results and discussion

3.1. Synthesis and characterization of the ligands

The ligands LH^2 and LH^3 were synthesized by applying a known synthetic procedure, first reported by Bhattacharya and co-workers, for LH^1 (Scheme 1) [19]. Thus the 2-carboxaldehydic derivatives of quinoline and thiophene were heated with 1,2-diaminoanthraquinone in $PhNO_2$ at 140 °C for 16 h. After cooling, the ligands were precipitated upon addition of diethyl ether and isolated by filtration as brown-coloured air-stable solids. No additional purification was necessary. The ligands were characterized using ^1H NMR, HR MS and UV–vis spectroscopy (the limited solubility prevented $^{13}C\{^1H\}$ NMR being obtained). The distinguishing features of the ^1H NMR studies revealed characteristic resonances associated with the imidazole-appended donor group (pyridine, quinoline or thiophene). For example, LH^3 (thiophene derivative) gave a signature 'doublet of doublets' resonance at 7.16 ppm, attributed to the thiophene proton at the 4-position, observed upfield from the starting carboxaldehyde precursor (cf. 7.24 ppm in $CDCl_3$). In all three ligands the proton resonances of the anthraquinone unit were weakly perturbed by the subtle electronic changes in imidazole character imposed by the pendant groups, suggesting an element of electronic communication throughout the ligand and across the imidazole unit.

Mass spectrometry (LR and HR) revealed the protonated parent ions $[M+H]^+$ in all cases. The unsymmetrical substitution pattern of the ligands could be expected to result in two unique carbonyl stretching frequencies as has been reported in highly resolved IR spectra for a range of substituted benzo- and naphthaquinones derivatives [23a]. The unsymmetrical nature of the ligands here could be further enhanced by intramolecular C=O•••H–N hydrogen bonding: a tautomeric form, which protonates the N in the 1-position, may allow such an arrangement, although the ring strain of the fused five-membered imidazole unit may discourage such an interaction. Solution state IR measurements confirmed the presence of the anthraquinone unit, with a distinct absorption observed for each ligand around 1610 cm^{-1} consistent with a C=O stretch (variation in the pendant group does not perturb the carbonyl frequency) [23b,c], with another feature at 1590 cm^{-1}, which is probably ν(C=C). The spectra were not obtained at sufficient resolution to allow further interpretation of these results.

3.2. Synthesis and characterization of the complexes

Two types of Ir(III) complex were isolated (Fig. 2) depending on the specific synthetic procedure adopted. Neutrally charged hetero-ligand complexes $[Ir(ppy)_2(L)]$ (where $L = L^1–L^3$) were isolated following addition of base (stoichiometric Na_2CO_3) to a reaction mixture composition of 2:1 ligand to $[(ppy)_2Ir(\mu\text{-}Cl_2)Ir(ppy)_2]$. Under these conditions product isolation with anionic L^3 suggests bidentate coordination *via* both the imidazole and thiophene units. A previous study has shown thiophene coordination to Ru(II) within a mixed phosphinoterthiophene ligand; importantly only strongly basic conditions (NaOH) induce cyclometallation allowing the coordination mode to be switched to C on the thiophene ring [24]. Of greater significance is a recent report of a related Ir(III) complex incorporating C,S-coordinated 2-phenylthiophene [25].

In this study the absence of base, followed by addition of an excess of NH_4PF_6, yielded the monocations $[Ir(ppy)_2(LH)][PF_6]$

Table 1
Selected bond lengths (Å) and angles (°) for $[Ir(ppy)_2(L^1)]$, $[Ir(ppy)_2(L^2)]$ and $[Ir(ppy)_2(LH^1)][PF_6]$.

Bond length (Å)/angle (°)	$[Ir(ppy)_2(L^1)]$	$[Ir(ppy)_2(L^2)]$	$[Ir(ppy)_2(LH^1)][PF_6]$
Ir(1)-N(1)	2.137(11)	2.239(6)	2.169(6)
Ir(1)–N(2)	2.131(11)	2.120(6)	2.132(6)
Ir(1)–N(4)	2.063(10)	2.066(6)	2.053(6)
Ir(1)–N(5)	2.058(10)	2.040(6)	2.047(6)
Ir(1)–C(2)	1.994(12)	2.022(8)	2.018(7)
Ir(1)–C(3)	2.014(13)	1.997(7)	2.009(7)
C(1)–N(2)	1.347(17)	1.364(9)	1.338(9)
C(1)–N(3)	1.307(16)	1.346(9)	1.363(9)
N(1)–Ir(1)–N(2)	76.0(4)	75.5(2)	76.0(2)
N(4)–Ir(1)–N(5)	173.9(4)	175.8(3)	174.3(2)

Table 2
Parameters associated with the single crystal diffraction data collection for $[Ir(ppy)_2(L^1)]$, $[Ir(ppy)_2(L^2)]$ and $[Ir(ppy)_2(LH^1)][PF_6]$.

	$[Ir(ppy)_2(L^1)]\cdot 2.5CHCl_3$	$[Ir(ppy)_2(L^2)]\cdot CH_3OH$	$[Ir(ppy)_2(LH^1)][PF_6]\cdot CH_3CN$
Empirical formula	$C_{42}H_{26}IrN_5O_2.2.5CHCl_3$	$C_{46}H_{28}IrN_5O_2.CH_3OH$	$C_{42}H_{27}IrN_5O_2.CH_3CN.PF_6$
Formula weight	1123.30	906.98	1011.91
Temperature	150(2) K	150(2) K	150(2) K
Wavelength	0.71073 Å	0.71073 Å	0.71073 Å
Crystal system	Triclinic	Triclinic	Monoclinic
Space group	P-1	P-1	P21/c
Unit cell dimensions	a = 13.0514(13) Å, α = 106.255(5)°	a = 12.2817(6) Å, α = 101.320(3)°	a = 8.7232(2) Å, α = 90°
	b = 13.6047(11) Å, β = 116.019(5)°	B = 13.2081(8) Å, β = 101.139(3)°	b = 41.5149(10) Å, β = 99.2580(10)°
	c = 14.7239(16) Å, γ = 92.472(6)°	C = 13.4335(5) Å, γ = 117.302(2)°	c = 10.9535(3) Å, γ = 90°
Volume	2213.4(4) $Å^3$	1795.62(15) $Å^3$	3915.06(17) $Å^3$
Z	2	2	4
Density (calculated)	1.685 Mg/m^3	1.677 Mg/m^3	1.717 Mg/m^3
F(000)	1102	900	1992
Crystal size	0.08 × 0.08 × 0.05 mm^3	0.10 × 0.04 × 0.04 mm^3	0.20 × 0.20 × 0.10 mm^3
Theta range for data collection	3.05–23.33°	2.94–27.53°	2.56–24.82°
All reflections	10,914	11,910	10,357
Independent reflections	6323	8203	6185
Observed reflections	4643	6316	4879
Goodness-of-fit on *F*	1.061	1.035	1.062
R_{int}	0.0992	0.0571	0.0441
Final *R* indices [$I > 2$sigma(I)]	$R1 = 0.0786$, w$R2 = 0.1647$	$R1 = 0.0596$, w$R2 = 0.1062$	$R1 = 0.0476$, w$R2 = 0.0887$
R indices (all data)	$R1 = 0.1116$, w$R2 = 0.1820$	$R1 = 0.0915$, w$R2 = 0.1196$	$R1 = 0.0702$, w$R2 = 0.0978$

(where $LH = LH^1$–LH^2). It was not possible, however, to isolate the complex $[Ir(ppy)_2(LH^3)][PF_6]$ using this methodology. Attempts yielded only $[Ir(ppy)_2(MeCN)_2][PF_6]$ (solvent for counter anion exchange is MeCN) as deduced by ^1H NMR, and indeed further reaction of $[Ir(ppy)_2(MeCN)_2][PF_6]$ with LH^3 in CH_2Cl_2 also failed to give the desired cationic product. It is possible therefore that the weaker donating ability of the thiophene unit can only be overcome and compensated for by a correspondingly harder donor at the imidazole group, thus requiring deprotonation.

The complexes were characterised in the solution state using ^1H NMR and, solubility permitting, ^{13}C–$\{^1H\}$ NMR spectroscopies, UV–vis absorption and luminescence spectroscopy. Additional data were provided *via* HR MS and IR with three examples yielding structural information *via* single crystal X-ray diffraction studies.

3.3. X-ray crystallography

Single crystals suitable for diffraction studies were isolated using vapour diffusion of Et_2O in to $CHCl_3$, CH_3OH or CH_3CN solutions of the complexes over a period of 24 h at room temperature. The parameters associated with the data collection are presented in Table 2 with selected bond lengths and angles (principally involving the coordination spheres) shown in Table 1.

The solid-state structural determinations (Figs. 3–5) support the proposed formulations determined from the solution state spectroscopic analyses. Each of the complexes revealed pseudo-octahedral coordination geometries with a chelated imidazolium ligand. As with numerous related examples of this type [26], the relative coordination geometry of the cyclometallated phenylpyridine ligands is retained from that of the precursor (*i.e. cis* C,C and *trans* N,N) [27]. It is noteworthy that when the pyridine pendant (L^1) is exchanged for quinoline (L^2) the Ir(1)–N(1) bond length increases, presumably due to the greater sterical requirements of the latter. Interestingly, changing the overall charge of the complex (confirmed by the presence or absence of PF_6^- counter anion) induces only subtle changes in the d(Ir–N) bond lengths, in fact d(Ir–N) (imidazole) does not change. However, within the imidazole unit, while C(1)–N(3) is shorter than C(1)–N(2) for the neutral complex, it is contrastingly longer within the cationic analogue.

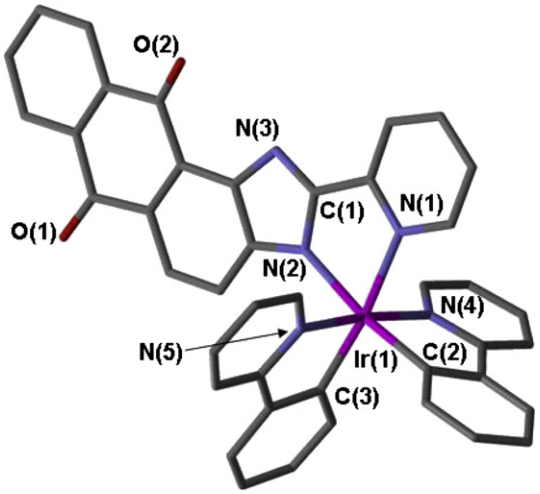

Fig. 3. The structure of $[Ir(ppy)_2(L^1)]$. Hydrogen atoms are omitted for clarity.

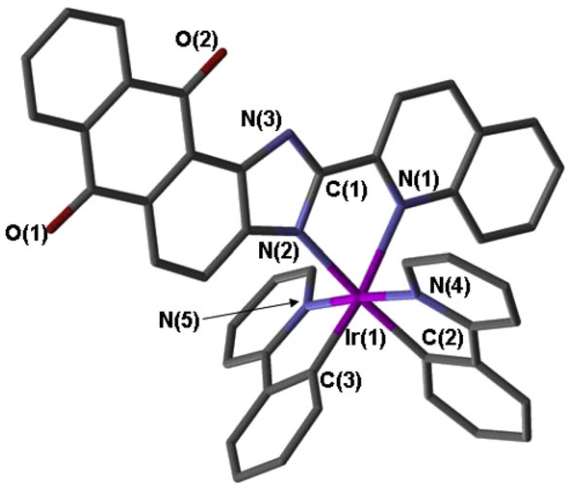

Fig. 4. The structure of $[Ir(ppy)_2(L^2)]$. Hydrogen atoms are omitted for clarity.

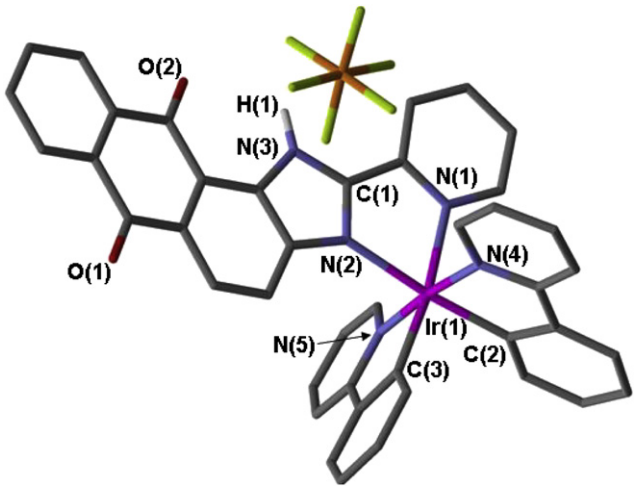

Fig. 5. The structure of $[Ir(ppy)_2(LH^1)][PF_6]$. All hydrogen atoms except H(1) are omitted for clarity.

3.4. Spectroscopic properties of ligands and complexes

The absorption properties of the ligands are dominated by a broad visible absorption around 390–410 nm attributed to ILCT transitions. Since the absorption transitions possess significant N-to-quinone CT character [28], the electronic nature of the pendant group should influence the positioning of the absorption. This is indeed observed with the (relatively) electron-poor pyridine/quinoline ligands (LH^1/LH^2) possessing similar absorption maxima (392 nm), but the electron-rich thiophene inducing a significant bathochromic shift (415 nm), consistent with increased N-to-quinone charge transfer character [28], together with a dramatic increase in molar absorption coefficient. Although the specific reasons for the latter observation are not clear in this context, thiophene groups have been utilised in light-harvesting arrays to improve absorption coefficients [29].

The complexes all absorb in the visible region (Fig. 6): the features are in the range 350–500 nm and are typically broad in appearance. In accordance with related complexes it is likely that these visible absorptions are composites of superimposed ^{1}MLCT-type transitions [26,30] and perturbed (anthraquinone) ligand-centred (ILCT) bands. Related $[Ir(ppy)_2(L)]^+$ compounds based on

Table 3
Room temperature absorption and emission properties of the free ligands and corresponding complexes.

Ligand/complex	Abs. λ_{max} (ε/M^{-1} cm^{-1})/nm	Em. λ_{max}/nm[a]	τ (ns) aerated	τ (ns) degassed
LH^1	392 (2800)	562	<5	–
LH^2	393 (1600)	565	<5	–
LH^3	415 (19,100)	553	<5	–
$[Ir(ppy)_2(L^1)]$	420 (12,600)	–[b]	–[b]	–[b]
$[Ir(ppy)_2(L^2)]$	433 (15,300)	616	94	121
$[Ir(ppy)_2(L^3)]$	397 (13,200)	558	<5	449
$[Ir(ppy)_2(LH^1)][PF_6]$	391 (16,100)	560	<5	<5
$[Ir(ppy)_2(LH^2)][PF_6]$	390 (23,300)	574	<5	947

[a] Excitation at 450 nm.
[b] Very weak.

functionalised 2,2′-bipyridyl ancillary ligands show that ^{1}LLCT transitions can also contribute in this region of the absorption spectra [31]. There was very little evidence for weaker absorptions >500 nm which may be due to spin forbidden absorptions associated with formation of ^{3}MLCT states [26,30]. The results for the complexes show that the absorption maxima for the cationic complexes $[Ir(ppy)_2(LH^1)][PF_6]$ and $[Ir(ppy)_2(LH^2)][PF_6]$ are blue-shifted, whereas deprotonation (and thus formation of the corresponding neutral complexes) causes a bathochromic shift in the most intense bands.

Luminescence measurements were conducted on MeCN solutions using 450 nm excitation of the longest wavelength absorption in each case (Table 3). The free ligands were firstly assessed, each displaying a short lived ($\tau < 5$ ns) broad fluorescence in the visible region *ca.* 550–560 nm, which is ascribed to an ILCT excited state and comparable to related amino-substituted anthraquinone species [32].

Both cationic complexes $[Ir(ppy)_2(LH^1)][PF_6]$ and $[Ir(ppy)_2(LH^2)][PF_6]$ displayed a broad, but relatively weak visible emission around 560–570 nm, consistent with an excited state of CT origin, which appeared comparable to the corresponding free ligands. The visible emission of $[Ir(ppy)_2(LH^2)][PF_6]$ was sensitive to dissolved oxygen since the lifetime was extended to 947 ns upon degassing the solution, suggesting a significant ligand-centred character in the excited state. Upon deprotonation, however, the complexes displayed more varied photophysical behaviour. Surprisingly, under aerated and de-aerated experimental conditions $[Ir(ppy)_2(L^1)]$ appeared to be too weakly emissive to allow

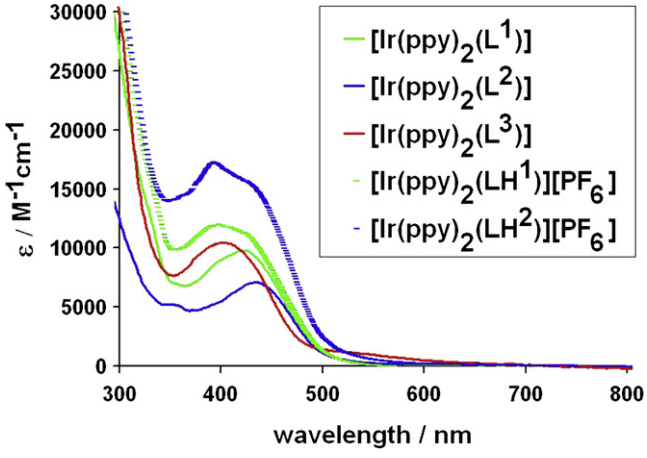

Fig. 6. UV–vis spectra for the complexes recorded in aerated MeCN at a concentration of 6.4×10^{-5} M.

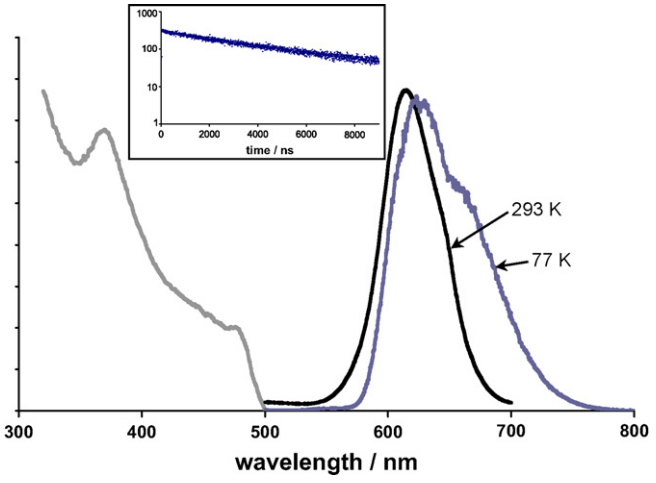

Fig. 7. Excitation (left) and emission (right) spectra at 293 (aerated MeCN) and 77 K (9:1 EtOH:MeOH glass) for $[Ir(ppy)_2(L^2)]$ (Inset: lifetime decay at 77 K; 3.79 μs).

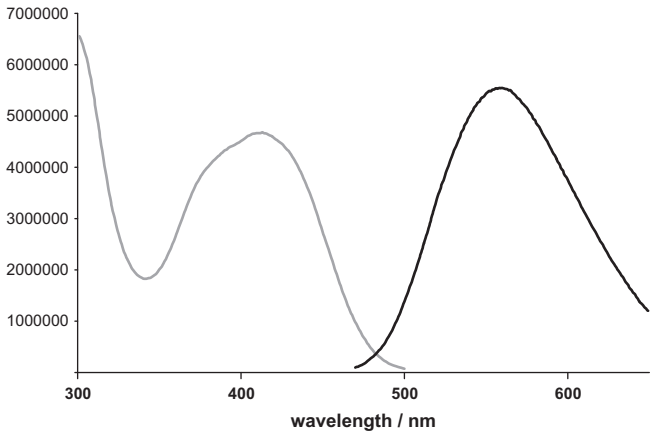

Fig. 8. Steady state excitation (left) and emission (right) spectra of [Ir(ppy)$_2$(L^3)] (aerated MeCN).

reliable measurement: the reasons for this are currently not known. In contrast, the quinoline analogue [Ir(ppy)$_2$(L^2)] displayed a broad emission with $\lambda_{max} = 616$ nm (Fig. 7) with a corresponding single exponential component lifetime of 94 ns in aerated MeCN. Cyclometallated Ir(III) complexes often display emission from either ^{3}MLCT or ^{3}IL [33] (mediated by very efficient spin-orbit coupling), the latter usually characterised by prominent vibronic features, as well as admixtures of the two. The emission profile, lifetime and relative insensitivity to dissolved oxygen of [Ir(ppy)$_2$(L^2)] is therefore more typical of a ^{3}MLCT-based phosphorescence [30]. Measurement at 77 K (EtOH/DCM/MeOH; 40/9/1 glass) revealed an emission profile that closely resembled that obtained at room temperature (a very minor shoulder was also present), suggesting that the origin of the emitting state is probably still dominated by ^{3}MLCT (perhaps with some ^{3}IL character [4]), and thus closely related to [Ir(ppy)$_3$] which also displays predominant ^{3}MLCT emission at 77 K [30]. The decay profile was fitted to a single exponential giving a lifetime of 3.79 μs that, again, corresponds well with an excited state of dominant ^{3}MLCT character. In contrast, the thiophene analogue [Ir(ppy)$_2$(L^3)] was emissive (Fig. 8) at 558 nm ($\tau < 10$ ns, aerated MeCN), and demonstrated sensitivity to dissolved oxygen ($\tau_{degas} = 449$ ns), which is indicative of a more ligand-centred dominated process.

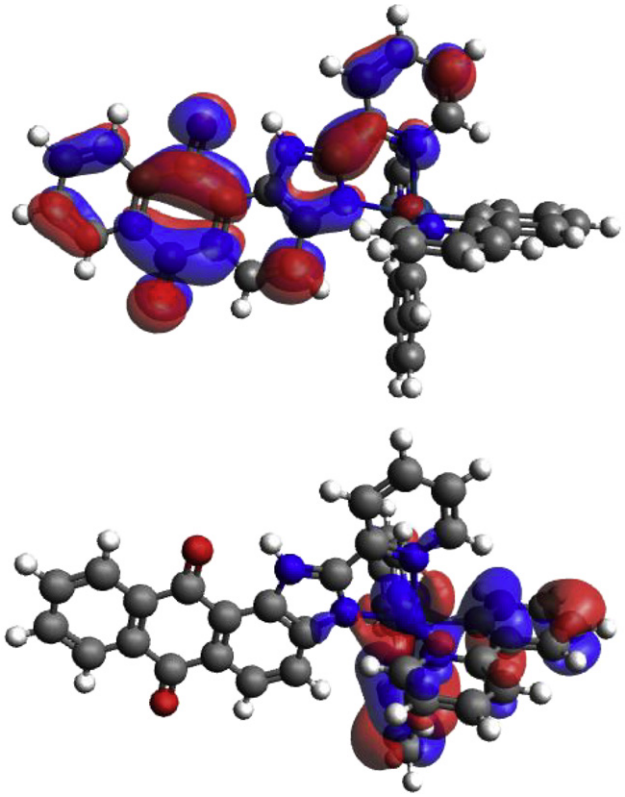

Fig. 9. HOMO (bottom) and LUMO (top) representations computed for [Ir(ppy)$_2$(LH^1)]$^+$.

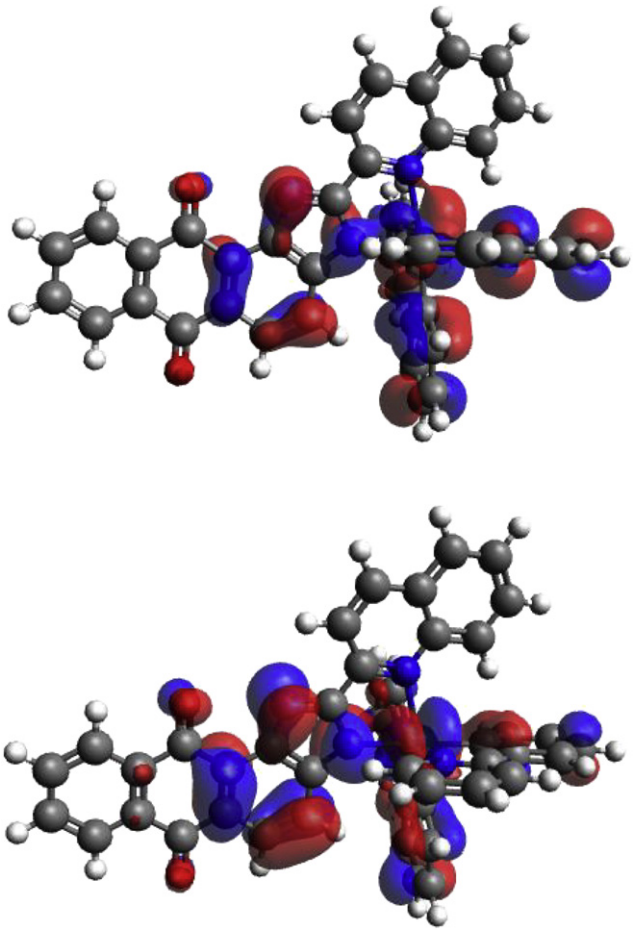

Fig. 10. HOMO (top) and HOMO-1 (bottom) representations computed for [Ir(ppy)$_2$(L^2)].

In the course of our measurements it was also observed that MeCN solutions of [Ir(ppy)$_2$(LH^2)][PF$_6$] slowly converted (over the course of about 28 days) to the neutral form (*i.e.* the imidazole NH is deprotonated) and therefore care should be taken when storing such species. Conversely *in situ* acidification of [Ir(ppy)$_2$(L^2)] did not produce spectroscopic evidence for [Ir(ppy)$_2$(LH^2)][PF$_6$], suggesting that the neutrally charged complexes retain reasonable stability in solution.

In an attempt to further elucidate the nature of the electronic transitions within these species, density functional theory (DFT) calculations (computed using the B3PW91 hybrid functional) were undertaken on four complexes: [Ir(ppy)$_2$(L^1)], [Ir(ppy)$_2$(LH^1)][PF$_6$], [Ir(ppy)$_2$(L^2)] and [Ir(ppy)$_2$(LH^2)][PF$_6$]. Such an approach has been demonstrated to be useful for determining the nature of electronic absorptions in related cyclometallated Ir(III) complexes [34], since experimental observations are often complicated, with an aim to informing the design of emissive materials [35]. However, whilst the accuracy of the orbital energies from calculations on complexes incorporating late transition metals is insufficient to warrant

a detailed discussion of the HOMO-LUMO energies (and their comparison with experimentally observed absorption energies), an analysis of the frontier orbitals nevertheless provides a qualitative insight into the observed lowest energy absorptions. Firstly, it is noteworthy than in all four cases the LUMOs are localised on the ancillary anthra[1,2-*d*]imidazole-6,11-dione-derived ligands (for example, Fig 9). Secondly, the protonation state of the imidazole portion of the ancillary ligand (and thus overall charge of the complex) appears to influence the nature of the HOMOs. In both neutral complexes, $[Ir(ppy)_2(L^{1/2})]$, several of the highest-energy occupied orbitals are sufficiently close in energy to be considered essentially isoenergetic ($\Delta E < 0.2$ eV). Therefore, for the neutral complexes, there is an ambiguity as to which MO is involved in the lowest energy absorption process. For $[Ir(ppy)_2(L^1)]$, the HOMO ($E = -5.44$ eV) is primarily associated with the Ir-phenyl moieties, whereas the HOMO-1 ($E = -5.61$ eV) is associated with the Ir(III) ion and L^1, consistent with accessible LLCT, MLCT and IL contributions, respectively. For $[Ir(ppy)_2(L^2)]$, both the HOMO ($E = -5.47$ eV) and HOMO-1 ($E = -5.63$ eV) (see Fig 10) are associated with Ir(III) and L^2, which is more consistent with greater MLCT character and therefore corroborates our experimental observations for this complex. In contrast, both of the cationic complexes $[Ir(ppy)_2(LH^{1/2})]^+$ possess HOMO, HOMO-1 and HOMO-2, which are all closely associated with the phenylpyridine ligands, suggesting that LLCT may predominate over IL character in the lowest energy absorption of these species.

4. Conclusions

This investigation demonstrates the synthetic application of condensing aldehydes with 1,2-diaminoanthraquinone to yield anthra[1,2-*d*]imidazole-6,11-dione-derived ligands and their resultant coordination chemistry with Ir(III). Importantly, in most cases the overall charge of the complex can be controlled *via* protonation/deprotonation of the imidazole moiety. However, in the case of the thiophene-appended complex deprotonation was required to induce chelation of the ligand. Crystallographic studies showed that the overall charge also subtly affects the bond distances within the imidazole unit (more so than those associated with the coordination sphere), but that the steric requirements of the pendant group (pyridine vs. quinoline) probably have a more profound influence on the strength of the ligand-metal interactions. In general, both the absorption and emission properties of the complexes are dominated by the coordinated anthra[1,2-*d*] imidazole-6,11-dione-derived ligands. Visible absorption (390–430 nm) is accompanied by short lived and/or weak emission at 550–575 nm. In this context $[Ir(ppy)_2(L^2)]$ is quite unique, displaying a longer-lived luminescence tentatively ascribed to a ^{3}MLCT excited emitting state. Supporting DFT calculations suggest that for these complexes the LUMO is always localised on the anthra[1,2-*d*]imidazole-6,11-dione-derived ligand, however, the predictions for the HOMOs appear dependent upon the charge and nature of the ligand.

Acknowledgements

The EPSRC are thanked for funding. Dr Robert Jenkins, Mr Robin Hicks and Mr David Walker are thanked for running low-resolution mass spectra. The staff of the EPSRC MS National Service (University of Swansea) are also gratefully acknowledged.

Appendix A. Supplementary material

Crystallographic data including bond lengths and bond angles associated with compounds $[Ir(ppy)_2(L^1)]$ (code: 776336) $[Ir(ppy)_2(L^2)]$ (code: 776337) $[Ir(ppy)_2(LH^1)](PF_6)$ (code: 776338) have been deposited with the CCDC and can be obtained free of charge via www.ccdc.cam.ac.uk/data_request/cif.

References

[1] (a) V.W.W. Yam, K.K.W. Lo, Coord. Chem. Rev. 184 (1998) 157;
M.W. Cooke, G.S. Hanan, Chem. Soc. Rev. 36 (2007) 1466;
(b) J.N. Demas, B.A. DeGraff, Coord. Chem. Rev. 211 (2010) 317;
(c) M. Bartholomii, J. Valliant, K.P. Maresca, J. Babich, J. Zubieta, Chem. Commun. (2009) 493;
(d) L. Fabrizzi, M. Liechelli, A. Taglietti, Dalton Trans. (2003) 3471;
(e) C.W. Tang, S.A. Van Slyke, Appl. Phys. Lett. 51 (1987) 913;
(f) E. Baranoff, J.H. Yum, M. Graetzel, M.K. Nazeeruddin, J. Organomet. Chem. 694 (2009) 2661;
(g) V. Fernandez-Moreira, F.L. Thorp-Greenwood, M.P. Coogan, Chem. Commun. 46 (2010) 186.
[2] (a) J.A.G. Williams, Chem. Soc. Rev. 38 (2009) 1783;
(b) L. de Cola, P. Belser, A. von Zelewsky, F. Vögtle, Inorg. Chim. Acta 360 (2007) 775;
(c) C.S.K. Mak, Q.Y. Leung, W.K. Chan, A.B. Djurišić, Nanotechnology 19 (2008) 424008.
[3] (a) H. Lin, M.E. Cinar, M. Schmittel, Dalton Trans. 39 (2010) 5130.(b) S.-K. Leung, K.Y. Kwok, K.Y. Zhang, K.K.-W. Lo, Inorg. Chem. 49 (2010) 4984;
(c) H. Sato, K. Tamura, M. Taniguchi, A. Yamagishi, New J. Chem. 34 (2010) 617;
(d) K.Y. Zhang, S.P.-Y. Li, N. Zhu, I.W.-S. Or, M.S.-H. Cheung, Y.-W. Lam, K.K.-W. Lo, Inorg. Chem. 49 (2010) 2530;
(e) E. Baranoff, J.-H. Yum, I. Jung, R. Vulcano, M. Grätzel, M.K. Nazeeruddin, Chem. Asian J. 5 (2010) 496.
[4] (a) M.A. Baldo, S. Lamansky, P.E. Burrows, M.E. Thompson, S.R. Forrest, Appl. Phys. Lett. 78 (2001) 1622;
(b) S. Lamansky, P. Djurovich, D. Murphy, F. Abdel-Razzaq, H.E. Lee, C. Adachi, P.E. Burrows, S.R. Forrest, M.E. Thompson, J. Am. Chem. Soc. 123 (2001) 4304.
[5] C.W. Tang, Coord. Chem. Rev. 215 (2001) 79.
[6] R.C. Evans, P. Douglas, C.J. Winscom, Coord. Chem. Rev. 250 (2006) 2093.
[7] (a) Q. Zhao, L. Li, M. Yu, Z. Liu, T. Yi, C. Huang, Chem. Commun. (2008) 685;
(b) Y. You, S.Y. Park, J. Am. Chem. Soc. 127 (2005) 12438;
(c) R.D. Costa, F.J. Céspedes-Guirao, E. Ortí, H.J. Bolina, J. Gierschner, F. Fernández-Lázaro, A. Sastre-Santos, Chem. Commun. (2009) 3886;
(d) C.H. Xu, W. Sun, C. Zhang, C. Zhou, C.J. Fang, C.H. Yan, Chem. Eur. J. 15 (2009) 8717;
(e) B. Du, L. Wang, H.B. Wu, W. Yang, Y. Zhang, R.S. Liu, M.L. Sun, J. Peng, Y. Cao, Chem. Eur. J. 13 (2007) 7432;
(f) C.J. Chang, C.H. Yang, K. Chen, Y. Chi, C.F. Shu, M.L. Ho, Y.S. Yeh, P.T. Chou, Dalton Trans. (2007) 1881.
[8] M.S. Lowry, S. Bernhard, Chem. Eur. J. 12 (2006) 7970.
[9] (a) Y.Y. Lyu, Y. Byun, O. Kwon, E. Han, W.S. Jeon, R.R. Das, K. Char, J. Phys. Chem. B 110 (2006) 10303;
(b) A.S. Ionkin, W.J. Marshall, D.C. Roe, Y. Wang, Dalton Trans. (2006) 2468.
[10] E.A. Plummer, A.V. Dijken, H.W. Hofstraat, L.D. Cola, K. Brunner, Adv. Funct. Mater. 15 (2005) 281.
[11] J.E. Jones, S.J.A. Pope, Dalton Trans. (2009) 8421.
[12] (a) Z. Yoshida, F. Takabayashi, Tet. Lett. 24 (1968) 913;
(b) T. Yamamoto, Y. Muramatsu, B.L. Lee, H. Kokubo, S. Sasaki, M. Hasegawa, T. Yagi, K. Kubota, Chem. Mater. 15 (2003) 4384.
[13] (a) M. Mehibel, S. Singh, E.C. Chinje, R.L. Cowen, I.J. Stratford, Mol. Cancer Ther. 8 (2009) 1261;
(b) M. Pickhardt, Z. Gazova, M. von Bergen, I. Khlistunova, Y.P. Wang, A. Hascher, E.M. Mandelkow, J. Biernat, E. Mandelkow, J. Biol. Chem. 280 (2005) 3628.
[14] (a) G. Zagotto, C. Sissi, L. Lucatello, C. Pivetta, S.A. Cadamurro, K.R. Fox, S. Neidle, M. Palumbo, J. Med. Chem. 51 (2008) 5566;
(b) M. Minunni, S. Tombelli, M. Mascini, A. Bilia, M.C. Bergonzi, F.F. Vincieri, Talanta 65 (2005) 578.
[15] (a) Y.X. Yuan, Y. Chen, Y.C. Wang, C.Y. Su, S.M. Liang, H. Cao, L.N. Ji, Inorg. Chem. Commun. 11 (2008) 1048;
(b) Y.X. Yuan, Y.C. Wang, L. Jiang, F. Gao, S.M. Liang, C.Y. Su, H. Cao, L.N. Ji, Aust. J. Chem. 61 (2008) 732.
[16] N.S. Bryce, J.Z. Zhang, R.M. Whan, N. Yamamoto, T.W. Hambley, Chem. Commun. (2009) 2673.
[17] Selected recent examples: (a) L.H. Fischer, M.I.J. Stich, O.S. Wolfbeis, N. Tian, E. Holder, M. Scaferling, Chem. Eur. J. 15 (2009) 10857;
(b) N. Zhao, Y.H. Wu, H.M. Wen, X. Zhang, Z.N. Chen, Organometallics 28 (2009) 5603;
(c) C.S.K. Mak, D. Pentlehner, M. Stich, O.S. Wolfbeis, W.K. Chan, H. Yersin, Chem. Mater. 21 (2009) 2173;
(d) F. Shao, J.K. Barton, J. Am. Chem. Soc. 129 (2007) 14733;
(e) F. Shao, B. Elias, W. Lu, J.K. Barton, Inorg. Chem. 46 (2007) 10187.
[18] (a) M.A. Nazif, J.-A. Bangert, I. Ott, R. Gust, R. Stoll, W.S. Sheldrick, J. Inorg. Biochem. 103 (2009) 1405;
(b) W.L. Jiang, Y. Gao, Y. Sun, F. Ding, Y. Xu, Z.Q. Bian, F.Y. Li, J. Bian, C.H. Huang, Inorg. Chem. 49 (2010) 3252;

(c) Q. Zhao, M.X. Yu, L.X. Shi, S.J. Liu, C.Y. Li, M. Shi, Z.G. Zhou, C.H. Huang, F.Y. Li, Organometallics 29 (2010) 1085;
(d) M.X. Yu, Q. Zhao, L.X. Shi, F.Y. Li, Z.G. Zhou, H. Yang, T. Yia, C.H. Huang, Chem. Commun. (2008) 2115;
(e) M. Dobroschke, Y. Geldmacher, I. Ott, M. Harlos, L. Kater, L. Wagner, R. Gust, W.S. Sheldrick, A. Prokop, Chem. Med. Chem. 4 (2009) 177.
[19] P. Chaudhuri, H.K. Majumder, S. Bhattacharya, J. Med. Chem. 50 (2007) 2536.
[20] M. Nonoyama, Bull. Chem. Soc. Jpn. 47 (1974) 767.
[21] SHELXL-PC Package. Bruker Analytical X-ray Systems, Madison, WI, 1988.
[22] M.J. Frisch, G.W. Trucks, H.B. Schlegel, G.E. Scuseria, M.A. Robb, J.R. Cheeseman, J.A. Montgomery Jr., T. Vreven, K.N. Kudin, J.C. Burant, J.M. Millam, S.S. Iyengar, J. Tomasi, V. Barone, B. Mennucci, M. Cossi, G. Scalmani, N. Rega, G.A. Petersson, H. Nakatsuji, M. Hada, M. Ehara, K. Toyota, R. Fukuda, J. Hasegawa, M. Ishida, T. Nakajima, Y. Honda, O. Kitao, H. Nakai, M. Klene, X. Li, J.E. Knox, H.P. Hratchian, J.B. Cross, V. Bakken, C. Adamo, J. Jaramillo, R. Gomperts, R.E. Stratmann, O. Yazyev, A.J. Austin, R. Cammi, C. Pomelli, J.W. Ochterski, P.Y. Ayala, K. Morokuma, G.A. Voth, P. Salvador, J.J. Dannenberg, V.G. Zakrzewski, S. Dapprich, A.D. Daniels, M.C. Strain, O. Farkas, D.K. Malick, A.D. Rabuck, K. Raghavachari, J.B. Foresman, J.V. Ortiz, Q. Cui, A.G. Baboul, S. Clifford, J. Cioslowski, B.B. Stefanov, G. Liu, A. Liashenko, P. Piskorz, I. Komaromi, R.L. Martin, D.J. Fox, T. Keith, M.A. Al-Laham, C.Y. Peng, A. Nanayakkara, M. Challacombe, P.M.W. Gill, B. Johnson, W. Chen, M.W. Wong, C. Gonzalez, J.A. Pople, Gaussian 03, Revision E.01. Gaussian, Inc., Wallingford CT, 2004.
[23] (a) M.L. Meyerson, Spectrochim. Acta 43A (1985) 1263;
(b) R.A. Walker, Spectrochim. Acta 27A (1971) 1785;
(c) N. Muthukumar, A. Ilangovan, S. Maruthamuthu, N. Palaniswamy, A. Kimura, Mater. Chem. Phys. 115 (2009) 444.
[24] C. Moorlag, O. Clot, M.O. Wolf, B.O. Patrick, Chem. Commun. (2002) 3028.
[25] X. Ren, D.J. Giesen, M. Rajeswaran, M. Madaras, Organometallics 28 (2009) 6079.
[26] S. Lamansky, P. Djurovich, D. Murphy, F. Abdel-Razzaq, R. Kwong, I. Tsyba, M. Bortz, B. Mui, R. Bau, M.E. Thompson, Inorg. Chem. 40 (2001) 1704.
[27] (a) K.A. McGee, K.R. Mann, Inorg. Chem. 47 (2008) 7800;
(b) H.S. Lee, S.Y. Ahn, H.S. Huh, Y. Ha, J. Organomet. Chem. 694 (2009) 3325;
(c) A.M. Talarico, I. Aiello, A. Bellusci, A. Crispini, M. Ghedini, N. Godbert, T. Pugliese, E. Szerb, Dalton Trans. 39 (2010) 1709;
(d) C.F. Li, G.P. Yong, Y.Z. Li, Inorg. Chem. Commun. 13 (2010) 179.
[28] P. Dahiya, M. Kumbhakar, D.K. Maity, T. Mukherjee, J.P. Mittal, A.B.R. Tripathi, N. Chattopadhyay, H. Pal, Photochem. Photobiol. Sci. 4 (2005) 100.
[29] (a) C.Y. Chen, M. Wang, J.Y. Li, N. Pootrakulchote, L. Alibabaei, C.H. Ngoc-Le, J.D. Decoppet, J.H. Tsai, C. Gratzel, C.G. Wu, S.M. Zakeeruddin, M. Gratzel, ACS Nano 3 (2009) 3103;
(b) Y. Cao, Y. Bai, Q. Yu, Y. Cheng, S. Liu, D. Shi, F. Gao, P. Wang, J. Phys. Chem. C 113 (2009) 6290.
[30] A. Tsuboyama, H. Iwawaki, M. Furugori, T. Mukaide, J. Kumatani, S. Igawa, T. Moriyaya, S. Miura, T. Takiguchi, S. Okada, M. Hoshino, K. Ueno, J. Am. Chem. Soc. 125 (2003) 12971.
[31] N. Zhao, Y.H. Wu, H.M. Wen, X. Zhang, Z.N. Chen, Organometallics 28 (2009) 5603.
[32] G.V. Kalyda, B.A.J. Jansen, P. Wielaard, H.J. Tanke, J. Reedijk, J. Biol. Inorg. Chem. 10 (2005) 305.
[33] (a) M.K. DeArmond, C.M. Carlin, Coord. Chem. Rev. 36 (1981) 325;
(b) P. Spellane, R.J. Watts, A. Vogler, Inorg. Chem. 32 (1993) 5633.
[34] For example: (a) T. Liu, B.H. Xia, X. Zhou, H.X. Zhang, Q.J. Pan, J.S. Gao, Organometallics 26 (2007) 143;
(b) I. Avilov, P. Minoofar, J. Cornil, L. De Cola, J. Am. Chem. Soc. 129 (2007) 8247.
[35] L. Shi, B. Hong, W. Guan, Z. Wu, Z. Su, J. Phys. Chem. A 114 (2010) 6559.